

## THEORY AND SIMULATION OF SPECTRAL LINE BROADENING BY EXOPLANETARY ATMOSPHERIC HAZE

Z. FELFLI,<sup>1,2</sup> T. KARMAN,<sup>3</sup> V. KHARCHENKO,<sup>1,4</sup> D. VRINCEANU,<sup>5</sup> J. F. BABB,<sup>1</sup> AND H. R. SADEGHPOUR<sup>1</sup>

<sup>1</sup> *ITAMP, Harvard-Smithsonian Center for Astrophysics, Cambridge, MA 02138*

<sup>2</sup> *Department of Physics, Clark Atlanta University, Atlanta, GA 30314*

<sup>3</sup> *Joint Quantum Centre, Durham University, Durham, DH1 3LE, United Kingdom*

<sup>4</sup> *Department of Physics, UConn, Storrs, CT 06269*

<sup>5</sup> *Department of Physics, Texas Southern University, Houston, TX 77004*

### ABSTRACT

Atmospheric haze is a leading candidate for opacity and lack of prominent features in exoplanetary spectra, as well as in the atmospheres of solar system planets, satellites, and comets. Exoplanetary transmission spectra, which carry information about how the planetary atmospheres become opaque to stellar light in transit, often show broad absorption in the region of wavelengths corresponding to spectral lines of sodium, potassium and water. We develop a detailed atomistic model, describing interactions of atomic or molecular radiators with dust and atmospheric haze particulates. This model incorporates a realistic structure of haze particulates from small nano-size seed particles up to sub-micron irregularly shaped aggregates and accounting for both pairwise collisions between the radiator and haze perturbers, and quasi-static mean field shift of atomic levels in haze environments. This formalism can explain large flattening of absorption and emission spectra in hazy atmospheres and shows how the radiator - haze particle interaction affects the absorption spectral shape in the wings of spectral lines and near their centers. The theory can, in principle, account for nearly all realistic structure, density, size and chemical composition of haze particulates. We illustrate the utility of the method by computing shift and broadening of the emission spectra of the Na D lines in haze environment, formed by Ar nano-clusters. Argon is used as the illustrative haze constituent only because of the simplicity of closed-shell atoms and their clusters for quantum mechanical calculations of interaction between radiator and nano-size haze particles. The elegance and generality of the proposed model should make it amenable to a broad community of users in astrophysics and chemistry.

*Keywords:* exoplanetary atmosphere — haze — pseudopotential — spectral shift and broadening

## 1. INTRODUCTION

Extrasolar planets (exoplanets) are being discovered at a breakneck pace, supplanting and transforming our understanding of planetary formation and habitability. Thousands of exoplanets have been identified using a host of detection techniques, through measurements of radial velocities, transits, and lensing (Explorer 2018; Encyclopaedia 2018). Many of these observed planets harbor atmospheres, and will be amenable to further observations with the launch of next generation telescopes, including the James Webb Space Telescope, the Transiting Exoplanet Survey Satellite, and with future terrestrial telescopes, including the Giant Magellan Telescope. An Analysis of spectral compositions and parameters of exoplanetary atmospheres is a topic of high interest, but prominent spectral features in observed transmission spectra of such exoplanets are often obscured.

Atmospheric haze is a leading candidate for the flattening of spectral transmission of exoplanetary occultation, a fact that is supported by observations of solar system planets, including Earth, and cometary atmospheres (Zhang et al. 2017; Deming & Seager 2017; Seager & Deming 2010). Spectra transmitted through hazy atmospheres carry information about how these atmospheres become opaque to stellar light in transit (Pont et al. 2008; Deming & Seager 2017; Spake et al. 2018). Recent laboratory experiments simulating hazy environments for super-Earths and mini-Neptunes atmospheres suggest that some of these atmospheres contain thick photochemically generated hazes (Hörst et al. 2018). Because hazy environments can reflect and absorb light, their conditions ought to be explored for direct imaging of exoplanets (Morley et al. 2015).

The stellar flux occultation during a planet's transit can also give clues to the persistence of an atmosphere; the wavelength dependent measurement of the planet transit depths reveal information on atmospheric atomic and molecular composition and transparency of the atmosphere. The Na I D and K I first resonance lines were modeled in absorption to constrain line-of-sight atmosphere barometric parameters and cloud depths (Seager & Sasselov 2000). Predictions made by (Seager & Sasselov 2000) were based on the assumption that these exoplanetary atmospheres are similar to brown and cool L dwarfs with similar effective temperatures. Water is expected to be the most spectroscopically active gas, but Na I, K I, metastable He I and CO have been identified in hot Jupiter atmospheres, and in particular in HD 209458b, HD 189733b, and WASP-103b (Seager & Deming 2010; Sing et al. 2011; Deming & Seager 2017; Spake et al. 2018; Pont et al. 2008, 2013; Lendl et al. 2017). Many of the detected lines are model dependent,

but Na I (and K I) resonant doublets are not, as there are no other absorbers at such wavelengths.

In methane dwarfs (Burrows et al. 2000, 2001), the K I doublet  $4^2S - 4^2P$  absorption line at 769 nm is broad and is responsible for large continuum depression, red shifted in optical spectra. The continuum broadening is induced due to collisional interaction (pressure broadening) between the radiator and background gas atoms and molecules. This lower than expected contrast of the strength of the alkali metal lines (Fortney et al. 2003) has been puzzling: subsolar elemental abundances, stellar radiation ionization, and atmospheric haze particulates have been invoked as sources for the diminished strength of the lines.

The haze hypothesis has gained currency (Burrows 2014; Deming & Seager 2017). Spectra observed from different planetary and exoplanetary atmospheres, comets, and natural satellites reveal unusual lack of sharp spectral features, attributed to the presence of atmospheric dust, ice and haze particles (Wong et al. 2003; Greenberg & Li 1999; West 1991; Ortiz et al. 1996; Rannou et al. 2002; West 1991; Tomasko et al. 1986). A compelling evidence for the direct role played by haze layers in flattening of the exoplanetary lines is the transit spectra of HD189733b in near-UV and mid-IR by Pont et al. (2013, 2008). Lack of features in the range from 550 to 1050 nm in the spectra of HD 189733b is suggestive of extinction by condensates high in the atmosphere (Pont et al. 2008). In general, hazes are mostly small (sub-micron) cluster particulates that can produce a broad continuum opacity to light. Interaction between haze particles and radiating atoms or molecules can dramatically modify absorption spectra of exoplanets. The red hue of Jupiter is likely produced by unidentified trace species (or haze) (Burrows 2014). The transit spectra for the mini-Neptune GJ 1214b have been shown by (Kreidberg et al. 2014) to be 5-10 times flatter than a water-rich, H<sub>2</sub>-dominated atmosphere, heralding the presence of a thick layer of haze, or other high molecular weight gas. *In situ* measurements of the effective density of aerosol materials in analogue Titan atmospheres confirm values of  $\sim 0.4 - 1.13 \text{ g/cm}^3$ , which for a methane dominated hazy environment, translates to atomic/molecular densities of a few times  $10^{22} \text{ cm}^{-3}$  (Hörst & Tolbert 2013).

We present a theoretical framework for a quantum mechanical description of the shift and broadening of atomic and molecular spectral lines by dust and haze particles at densities relevant to hazy planetary atmospheres. Our model can be applied to shift and broadening analysis of different lines of atomic and molecular spectra, when haze particulates have liquid or solid

structures or consist of high porosity materials (Vinatier et al. 2018). Spectral calculations are obtained through the introduction of the pseudo-potential for the interaction between radiator electrons and atoms and molecules of haze particles (Szasz 1985). The pseudo-potential method allows us to carry out calculations for different chemical compositions of haze (Jacquet et al. 2011; Boatz & Mario 1994). The binary collision between the radiator and haze particulate, affecting the radiator line center, is also considered (Allard & Kielkopf 1982).

## 2. METHODOLOGY

### 2.1. Modeling of Emission and Absorption Spectra in Haze Environments

The physical nature, composition and structure of these particles is roughly known for the Earth, some solar system planets, satellites, and comets (Greenberg & Li 1999; West 1991; Seignovert et al. 2017), but for exoplanetary atmospheres the nature of the particles is not known (Tinetti et al. 2007). Analysis and interpretation of atomic and molecular spectra observed from dusty environments is a formidable task because of complicated quantum mechanical interaction between radiating atoms/molecules and haze particles.

Another fundamental obstacle in modeling properties of mesoscopic dust, ice and haze particles is the stochastic nature of the haze particle distribution (Greenberg & Li 1999; Sciamma-O'Brien et al. 2012). A review on cloud modeling, and scattering and extinction efficiencies of cloud particles in terrestrial, giant gas giants, and brown dwarfs is given in (Marley 2013). The simplest approaches to modeling distributions employ empirically assigned refractive indices using the classical Mie model for scattering and absorption of radiation by spherical haze particles (Lenoble et al. 2013; Seignovert et al. 2017). This model fails to describe realistic changes in atomic and molecular emission/absorption spectra because optical properties of nano-size particles cannot be described by macroscopic parameters such as the refractive index.

### 2.2. Quantum Mechanical Model of Interaction Between Radiator and Haze Particles

The electronic Hamiltonian  $H_{el}$  for the radiator-haze system can be written as:

$$H_{el} = H_r + H_{hp} + V_{r-hp}, \quad (1)$$

where  $H_r$  is an electronic Hamiltonian of radiating atom or molecule;  $H_{hp}$  the haze particle Hamiltonian, and  $V_{r-hp}$  the potential of interaction between the haze and radiator electrons. The haze particle Hamiltonian  $\hat{H}_{hp}$

includes kinetic energies and interaction potential energies of all atomic and molecular constituents.

The term  $V_{r-hp}$  is given by the sum of interaction potential energies  $V_i$  between radiator electrons and an atomic or molecular constituent in the haze at location  $\mathbf{R}_i$  :  $V_{r-hp} = \sum_{i=1}^N V_i(\mathbf{r}_e, \mathbf{R}_r, \mathbf{R}_i)$ , where  $N$  is the total number of haze atoms and/or molecules,  $\mathbf{r}_e$  is the electron coordinate from the radiator center  $\mathbf{R}_r$ . Figure 1 illustrates the basic configuration of the haze-radiator system.

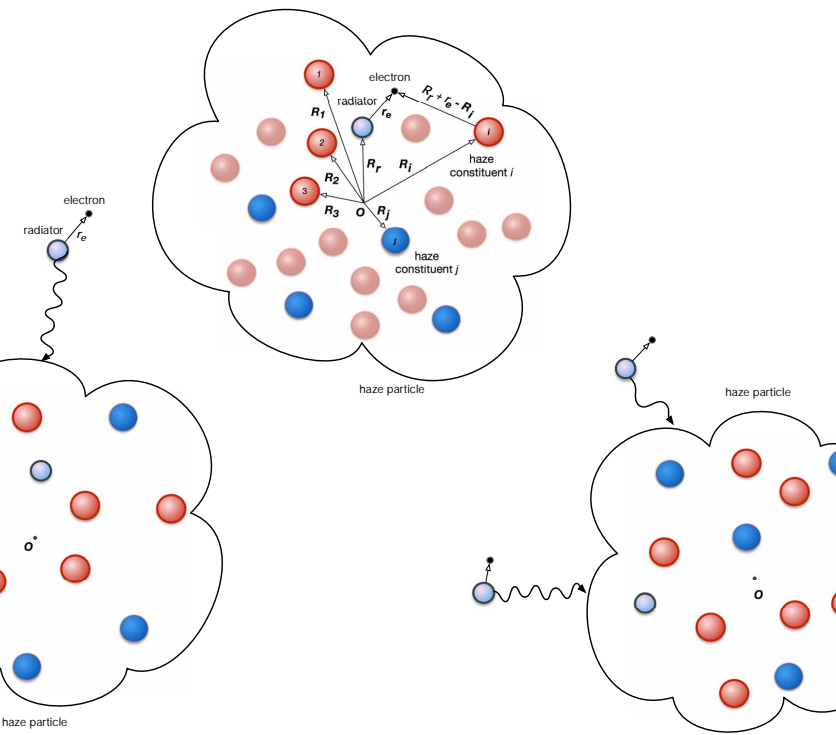


**Figure 1.** A diagram of haze particles of arbitrary shape interacting with radiator atoms. The active radiator electron,  $\mathbf{r}_e$ , interacts with the radiator core,  $\mathbf{R}_r$ , and with all other atoms within the haze at positions  $\mathbf{R}_i$ . Haze constituents of different chemical compositions are denoted with red and blue spheres. The density of haze atomic/molecular constituents is denoted by  $\rho(R_{i,j})$ , and Gaussian distributed in this work. Photons are indicated with wiggly arrows.

There are only dozens of atoms or molecules in nano-size seed particles and millions in sub-micron haze aggregates. The set of location vectors  $\{\mathbf{R}_i\}$  determines the geometrical structure of haze, its physical properties and characteristics of interaction with radiator. For mesoscopic size “haze-radiator” system, the set  $\{\mathbf{R}_i\}$  has typically an irregular structure and resembles an amorphous or liquid cluster. Nevertheless, seed particles could be represented by nano-crystals or amorphous Si

or C materials covered by polycrystalline structures of H<sub>2</sub>O and CO<sub>2</sub> ices or CH<sub>4</sub> droplets expected as outer shells in highly porous sub-micron haze aggregates.

### 2.2.1. Mean-field spectral line shift in haze environment

The atmospheric distribution of haze particles is non-uniform as is the distribution of atoms and molecules inside haze droplets. Our modeling of spectral line shift and broadening is focused on the quantum mechanical description of the interactions between the haze particles and the atomic or molecular radiators. The many-body interaction between the emitter and haze constituents is considered in the mean-field approximation.

The Fermi pseudopotential method (Fermi 1934) was first developed to describe species-dependent mean field pressure shift and broadening of Rydberg lines in gaseous environments and more recently in the context of Rydberg molecule formation in ultracold quantum gases (Greene et al. 2000).

The Fermi pseudopotential is defined is proportional to the scattering length  $L_i$  of the radiator electron from the  $i$ -th haze perturber (Fermi 1934), see Fig. 1,

$$V_i(\mathbf{r}_e, \mathbf{R}_r, \mathbf{R}_i) = \frac{2\pi\hbar^2}{m_e} L_i \delta(\mathbf{R}_r + \mathbf{r}_e - \mathbf{R}_i) \quad (2)$$

where  $\mathbf{r}_e$  is the radiator electron coordinate,  $L_i$  is the scattering length of the electron of mass  $m_e$  colliding with the haze atom/molecule at  $\mathbf{R}_i$ ,  $\hbar$  is the reduced Planck constant, and  $\delta()$  is the Dirac delta-function. The chemical composition of haze particles is represented by a set of individual scattering lengths  $\{L_i\}$ . The scattering length is obtained from the zero-energy limit of the scattering phase shift. Presence of perturbers in the vicinity of radiator modifies the radiator wave function and energy spectra that finally leads to changes in energy and rates of emitted/absorbed photons.

Models of spectral shift and broadening (Allard & Kielkopf 1982; Szudy & Baylis 1996) describe the influence of collisional or quasi-static interaction potentials on emission and absorption spectra. In the quasi-static approach, the line shift  $\Delta\omega = \omega - \omega_0$  induced in binary interaction is equal to the difference of radiator electron energies as a function of the perturber-radiator distance, i.e.  $\hbar\Delta\omega = \Delta V(R)$ , where  $\Delta V(R)$  is the difference of the ground and excited Born-Oppenheimer potential energies, e.g. Sec. 2, induced by the perturber. The inverted equation  $R_C = R(\Delta\omega)$  yields the location of Condon points, resulting in specific frequency shifts  $\Delta\omega$ . For the simplest case of cold and dilute gas of uniformly distributed perturbers, the intensity of the spectral line is proportional to the probability to find

a perturber at distances between  $R$  and  $R + dR$ , i. e.  $I(\Delta\omega) = 4\pi\rho R^2(\Delta\omega) |\frac{dR(\Delta\omega)}{d(\Delta\omega)}|$ , with  $\rho$  the perturber density (Allard & Kielkopf 1982). Haze particles and aggregates may be considered as an environment of slow perturbers with a large and essentially non-uniform perturber density  $\rho(R)$ .

The mean-field model in this work, is also applicable to calculations of collisional shift and broadening inside haze aggregate particles with high levels of porosity ( $\sim 90\%$ ). Collisional and mean field mechanisms dominate in different regions of emission and absorption spectra. Interaction between haze particles and radiator can provide significant shifts of atomic and molecular lines, in extreme cases up to  $10^4$  cm<sup>-1</sup> (Jacquet et al. 2011) depending on the radiator position.

Analytical formulas for the shifted electron energies  $\epsilon_{i,f}(\mathbf{R}_r)$  of a radiator in the ground (initial) and excited (final) states obtained from the leading term of the perturbation theory:

$$\epsilon_{i,f}(\mathbf{R}_r) = \epsilon_{i,f}^0 + \langle \Psi_{i,f}(\mathbf{r}_e) | V_{i,f} | \Psi_{i,f}(\mathbf{r}_e) \rangle = \epsilon_{i,f}^0 + \frac{2\pi\hbar^2}{m_e} \sum_{i=1}^N L_i |\Psi_{i,f}(\mathbf{r}_e)|^2 \quad (3)$$

where  $\Psi_i$  and  $\Psi_f$  are wave functions of the ground and excited states of free (unperturbed) radiator atoms and  $\epsilon_{i,f}^0$  are related electronic energies. For systems with high densities of perturbers, such as haze ice, dust or liquid droplets, the perturbation can be strong and radiator electronic wave functions need be renormalized according to the mean field induced by the perturbers (Demkov & Ostrovskii 1988). For haze particles and aggregates with a large number of equivalent atoms or molecules  $N$ , the summation in Eq. 3 can be replaced with integration over the volume of the haze aggregate with a specific volume density  $\rho(\mathbf{R})$ . For a collection of  $N$  identical perturbers, the Born-Oppenheimer electronic energies of the radiator  $\epsilon_{i,f}$  for initial  $i$ - and final  $f$ -states are calculated as:

$$\epsilon_{i,f}(\mathbf{R}_r) = \epsilon_{i,f}^0 + V_{i,f}(\mathbf{R}_r) = \epsilon_{i,f}^0 + \frac{2\pi\hbar^2}{m_e} L_i N \int d\mathbf{r}_e \rho(\mathbf{r}_e + \mathbf{R}_r) |\Psi_{i,f}(\mathbf{r}_e)|^2 \quad (4)$$

where  $\rho(\mathbf{R}_p)$  is the unit normalized spatial distribution function in the haze droplet at  $\mathbf{R}_p = \mathbf{r}_e + \mathbf{R}_r$ . The mean-field potential  $V_{i,f}(\mathbf{R}_r)$  induced by the haze particles depends on the symmetry of electronic states and symmetry of the perturber distribution function  $\rho(\mathbf{R}_p)$ . This potential can be a function of the radiator coordinate  $\mathbf{R}_r$ . The spectral intensity  $I(\Delta\omega)$  is expressed via mean-field energy shifts:

$$I(\Delta\omega) = \int d^3 R_r p(\mathbf{R}_r) \delta(\Delta\omega - [V_f(\mathbf{R}_r) - V_i(\mathbf{R}_r)])/\hbar \quad (5)$$

where  $p(\mathbf{R}_r)$  is the unit normalized distribution function of radiators inside and outside haze droplet. The replacement of  $p(\mathbf{R}_r)$  with the radiator partition function can provide a temperature dependence of the radiator spatial distribution. Angular anisotropy of the mean-field potentials  $V_{i,f}(\mathbf{R}_r)$  plays an important role in integration of the  $\delta$ -function in Eq. 5. For spherically symmetric Born-Oppenheimer energy splitting  $\Delta V(R_r) = V_f(\mathbf{R}_r) - V_i(\mathbf{R}_r)$ , the expression for  $I(\Delta\omega)$  formally reduces to the known approximation (Allard & Kielkopf 1982).

### 2.2.2. Shift and broadening of spectral line in binary collisions

The mean-field spectral shift represents only a part of the total shift and broadening of unperturbed spectral line with frequency  $\omega_0 = \Delta\epsilon_0 = \epsilon_i^0 - \epsilon_f^0$ . Collisional effects are thermally driven, and hence temperature dependent. In the relatively dense environments, the binary collision between the radiator and a nearby perturber happens in the presence of mean-field shifts induced by large number of other slowly moving perturbers. The temperature-dependent binary collision broadening and shift rates are, respectively  $\rho(\mathbf{R}_r)\gamma(T)$ , and  $\rho(\mathbf{R}_r)\sigma(T)$  (Allard & Kielkopf 1982; Vrinceanu et al. 2004).

The overall line shape is obtained upon integrating the localized contributions over the whole volume, assuming that the radiator is found at position  $\mathbf{R}_r$  with the spherically symmetric probability density  $p(\mathbf{R}_r)$ :

$$I(\omega) = \frac{1}{\pi} \int_0^\infty \frac{\rho(\mathbf{R}_r)\gamma}{[\omega - (\Delta\epsilon_0 + V_f(\mathbf{R}_r) - V_i(\mathbf{R}_r)) - \rho(\mathbf{R}_r)\sigma]^2 + [\rho(\mathbf{R}_r)\gamma]^2} \quad (6)$$

In the above, the first term in the denominator describes the shift of the resonance frequency  $\omega_0$ , and the second term the broadening.

We expect a strong transformation of the emission spectra when the radiator is localized near the surface or inside haze aggregate. In such cases, the strong mean-field interaction creates a broad emission/absorption spectra, significantly shifted from the unperturbed line at  $\omega_0$ . The spectral regions with the photon frequencies near the unperturbed spectral lines are mostly formed by collisional interactions with shifted and broadened Lorentzian profiles (Vrinceanu et al. 2004; Szudy & Baylis 1996), and become temperature dependent.

The rich experimental and theoretical database on collisional transformation of emission and absorption spectra are available for different atomic and molecular radiators in a gas environment (Szasz 1985; Vrinceanu et al. 2004), where physics of shift and broadening of spectra near the radiator spectral core is described by binary col-

lisions between radiators and gas particles. Analysis of spectral line shift and broadening provides valuable information on parameters of atmospheric gases and haze particles. Parameters of the collisional and mean-field mechanisms of the shift and broadening for different spectral lines can yield unique vistas on physical characteristics of haze particle size, shape and material.

## 3. ILLUSTRATIVE RESULTS

Compositions and parameters of haze particle and atmospheric gases are expected to vary considerably for different exoplanets. Nevertheless, the influence of haze nano-particles on spectra has certain common features despite specific properties of exoplanetary and planetary atmospheres. These common characteristics reflect the quantum-mechanical nature of interaction between radiator and nano-size objects and, with for illustrative purposes, can be investigated for the simplest haze environment: cool noble gas with embedded atomic nano-size atomic droplets and clusters, such as  $\text{He}_N$ ,  $\text{Ne}_N$ ,  $\text{Ar}_N$ , and  $\text{Xe}_N$ . We demonstrate the utility of the current theoretical framework for hazy exoplanetary atmospheres, using a sodium atom as the resonant radiator and argon as the haze constituent at realistic measured haze particle densities. We emphasize that while no haze constituents in Titan or exoplanetary atmospheres are made of Ar, the simplicity afforded by using closed-shell atoms, such as argon, of complex quantum mechanical Born-Oppenheimer potential energy curves, e. g. Fig. 2, serves to quantitatively illustrate the different shift mechanisms at play. Furthermore, argon nanoclusters are more readily accessible in the lab.

The electron scattering length for argon has been measured from low-energy drift velocities of electrons in an H-Ar mixture, to be  $L_{\text{Ar}} = -1.46 a_0$ , (Petrovic et al. 1995), where  $a_0$  is the Bohr radius. Admittedly, the haze constituency will more likely be in the form of carbon-bearing, water, and other complex molecules, but for purposes of computational efficiency, interacting sodium atoms with rare-gas atomic samples offers a convenient way to calculate the many-body mean-field aspect of this theory. Below, first we describe how we calculate the binary interaction in Na-Ar.

### 3.1. Binary Potential Energy Curves

We employ effective core potentials (ECPs), developed by Nicklass et al. (1995), to represent the 10 core electrons for argon and sodium atoms. The sodium core dipole polarizability is  $\alpha = 0.9947$  and exponential cut-off parameter  $\delta = 0.62$ , in atomic units, using the core polarization potentials (CPPs) developed by Fuentealba et al. (1982) and implemented in MOLPRO (Werner &

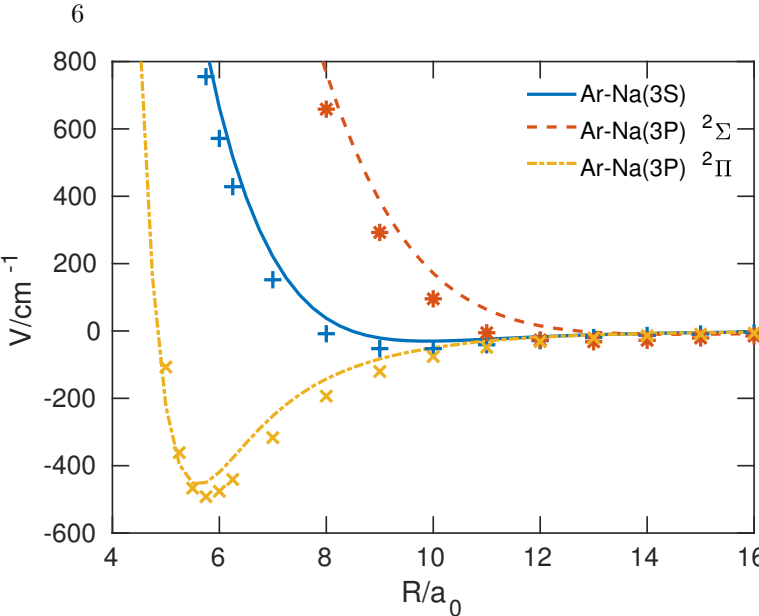


**Figure 2.** Potential energy curves for Ar–Na(3S,3P). The Na D line energy is subtracted. Lines correspond to the potential energy curves calculated in this work, and symbols correspond to calculated potential energy values (Saxon et al. 1977).

P. J. Knowles *et al.* 2012). The one-electron basis set for the valence electrons of the argon perturber is taken from (Nicklass et al. 1995). The sodium radiator is described using an extended one-electron basis set, defined as follows: The *s*, *p*, and *d* orbitals are represented by a set of uncontracted 5 Gaussians with even-tempered exponents between 1.0 and 0.01 atomic units. Two sets of uncontracted Gaussian *f* orbitals with exponents 0.08. and 0.008 are also included.

We perform complete active space self-consistent field (CASSCF) calculations to obtain molecular orbitals, state-averaged over the 3S ground state and 3P excited states. The active space contains the nine valence electrons in argon and sodium 3s and 3p orbitals. Subsequently, we perform multi-reference configuration interaction (MRCI) calculations, which include single and double excitations from this active space. The Pople size-consistency correction is added, and the interaction energies are calculated using the counterpoise procedure of (Boys & Bernardi 1970), to correct for the basis set superposition error. We use a dense grid in the radial coordinate, extending from  $R = 3$  to  $20 a_0$  in steps of  $0.25 a_0$ , with additional points at  $22, 25 a_0$ . A final point at  $R = 50 a_0$  is used to subtract any remaining error in size consistency. All calculations are performed using the MOLPRO suite of *ab initio* programs (Werner & P. J. Knowles *et al.* 2012).

The potential energy curves are shown in Fig. 2. Results obtained in this work are shown as lines. There are

two potentials correlating to the Na(3P) excited state. The  $^2\Sigma$  ( $^2\Pi$ ) potential governs the interaction if the excited valence electron occupies a 3P orbital oriented parallel (perpendicular) to the interatomic axis. The  $^2\Pi$  excited state potential is significantly more attractive, with a well depth of around  $450 \text{ cm}^{-1}$ , and becomes repulsive only for much shorter interatomic separations. The  $^2\Sigma$  excited state, however, has a more repulsive potential than the ground state. The calculated potentials are in good qualitative agreement with the results of Saxon et al. (1977).

### 3.2. Shift and broadening of Na line in Ar haze

The argon droplet is modeled by a Gaussian distribution, given by a spherically-symmetric position dependent density  $\rho(R) = [N_{\text{Ar}}/(2\pi a^3)^{3/2}] \exp(-R^2/2a^2)$ , which depends on the droplet size parameter  $a$ , and the number of Ar atoms,  $N_{\text{Ar}}$ . A sodium atom at a distance  $R_r$  from the center of the droplet has a shifted Lorentz absorption profile as in Eq. 6, where the shape of the line is determined by two contributions: a) mean field quasi-static contribution of neighboring argon atoms that produce the energy shifts  $\Delta V(R_r) = V_{3P}(\mathbf{R}_r) - V_{3S}(\mathbf{R}_r)$ , and b) collisional broadening  $\Gamma$  and shift  $\Sigma$  rates that are proportional to the local density:  $\Gamma = \rho(R_r)\gamma$  and  $\Sigma = \rho(R_r)\sigma$ . In this model, we use the measured values  $\gamma = 1.47 \times 10^{-20} \text{ cm}^{-1}/\text{cm}^{-3}$ , and  $\sigma = 0.75 \times 10^{-20} \text{ cm}^{-1}/\text{cm}^{-3}$  at  $T = 475 \text{ K}$  (Allard & Kielkopf 1982). For  $T = 2000 \text{ K}$ , we multiply the shift and broadening by a factor 1.4; this factor is obtained from a comparison of line broadening in Na-Ar collision from Jongerius et al. (1981).

Fig. 3 illustrates the absorption spectral line shape of the Na D line embedded in a haze environment of specific Ar density. The two cases considered, with 1000 and 10000 Ar atoms, include haze seed particles of size given by  $a = 40 \text{ a.u.}$  Because of the strong mean field interaction the line is extremely broad. For comparison, the line profile due to gaseous broadening is represented by the vertical dashed line, since the wavelength width  $\Delta\lambda/\lambda_0 \approx n\gamma/\Delta E$  is extremely small at this scale. In a typical planetary atmospheric application  $n = 10^{14} \text{ cm}^{-3}$ ,  $\gamma$  is in the range of  $10^{-20} \text{ cm}^{-1}/\text{cm}^{-3}$  (Allard & Kielkopf 1982; Jongerius et al. 1981) and  $\Delta E = 16964 \text{ cm}^{-3}$  for sodium atom, so that  $\Delta\lambda/\lambda_0 \sim 10^{-10}$ .

The probability of finding the sodium atom at some distance  $R_r$  is given by the Boltzmann distribution,  $p(R_r) = \frac{1}{Z} e^{-\epsilon_{3S}(R_r)/k_B T}$ , with normalization  $Z = \int_0^\infty e^{-\epsilon_{3S}(R_r)/k_B T} (4\pi R_r^2) dR_r$ ,  $\epsilon_{3S}(R_r)$  is the mean-field shift in the 3S state, see also Fig. 4, and  $k_B$  the Boltzmann constant. In the absence of core broadening due to binary collisions, the spectral line profile will

contain a characteristic discontinuity at the Na line. The line profiles are asymmetric about the radiator line center; this is an expectation of the change in sign of  $\Delta\epsilon(R)$ , see Fig. 4. *In situ* simulated laboratory measurements of Titan atmospheric aerosol density confirm that effective atomic/molecular densities of aerosol/haze are a few times  $10^{22} \text{ cm}^{-3}$  for a methane haze (Hörst & Tolbert 2013), in accord with our illustrative haze particle densities.

#### 4. DISCUSSION

Haze influence on absorption/emission spectra strongly depends on mixing ratios of haze particles in atmospheric regions responsible for the formation of transit spectra. The average frequency of the radiator binary collisions with atoms and molecules of ambient gas  $\nu_{\text{gas}} = n_{\text{gas}} v_r \sigma_{\text{gas}}$  is usually much larger than the haze-radiator collisional frequency  $\nu_{\text{haze}} = n_{\text{haze}} v_r \sigma_{\text{haze}}$ , because the number density of haze particles  $n_{\text{haze}}$  is much smaller than the gas number density  $n_{\text{gas}}$ . Here,  $v_r$  is the radiator velocity and  $\sigma_{\text{haze}}$  and  $\sigma_{\text{gas}}$  are, respectively, the radiator collisional cross section with haze and gas particles. Spectral intensities  $I_{\text{gas}}(\Delta\omega)$  and  $I_{\text{haze}}(\Delta\omega)$  induced by these two types of collisions are proportional, respectively, to related collisional frequencies  $\nu_{\text{gas}}$  and  $\nu_{\text{haze}}$ , and for  $\nu_{\text{gas}} \gg \nu_{\text{haze}}$ , the role of haze-radiator collisions are negligible. Nevertheless, huge shifts of electronic levels in haze/radiator interaction and collisions can provide a dramatic increase of the intensity of spectral wings comparing to the spectra induced in collisions with atmospheric gas. For example, spectra of atomic species, such as Na, K, Fe, Mg, S and others, can be mostly determine by the radiator interaction with haze nano-particles, if we consider spectral regions of large frequency shift  $\Delta\omega = |\omega - \omega_0| \gg \Gamma_{\text{gas}} \sim \nu_{\text{gas}}$  (Allard & Kielkopf (1982)). Collisions with the gas particles provide mostly small changes of the frequency near the line center, and the probability  $p_{\text{gas}}(\Delta\omega)$  to find a large shift  $\Delta\omega \gg \Gamma_{\text{gas}}$  can be estimated using the spectral Lorentzian width:  $p_{\text{gas}}(\Delta\omega) \sim \Gamma_{\text{gas}}/\Delta\omega \ll 1$ . To estimate the spectral intensity ratio  $\xi = I_{\text{gas}}(\Delta\omega)/I_{\text{haze}}(\Delta\omega)$ , we make a simplified, and realistic, assumption: a large frequency shift occurs in every haze-radiator collision and the probability of the large frequency shift  $\Delta\omega$  in haze collisions  $p_{\text{haze}}(\Delta\omega) \sim 1$ .

The spectral intensity ratio  $\xi(\Delta\omega)$  can be evaluated as:

$$\xi = \left( \frac{\nu_{\text{gas}} p_{\text{gas}}(\Delta\omega)}{\nu_{\text{haze}} p_{\text{haze}}(\Delta\omega)} \right) = \left( \frac{n_{\text{gas}}^2}{n_{\text{haze}} n_{\text{atomic}}^{\text{haze}}} \right) \left( \frac{\sigma_{\text{gas}}}{\sigma_{\text{haze}}} \right) \left( \frac{m_e v_r \sigma_{\text{gas}}}{\beta 2\pi L \hbar} \right), \quad (7)$$

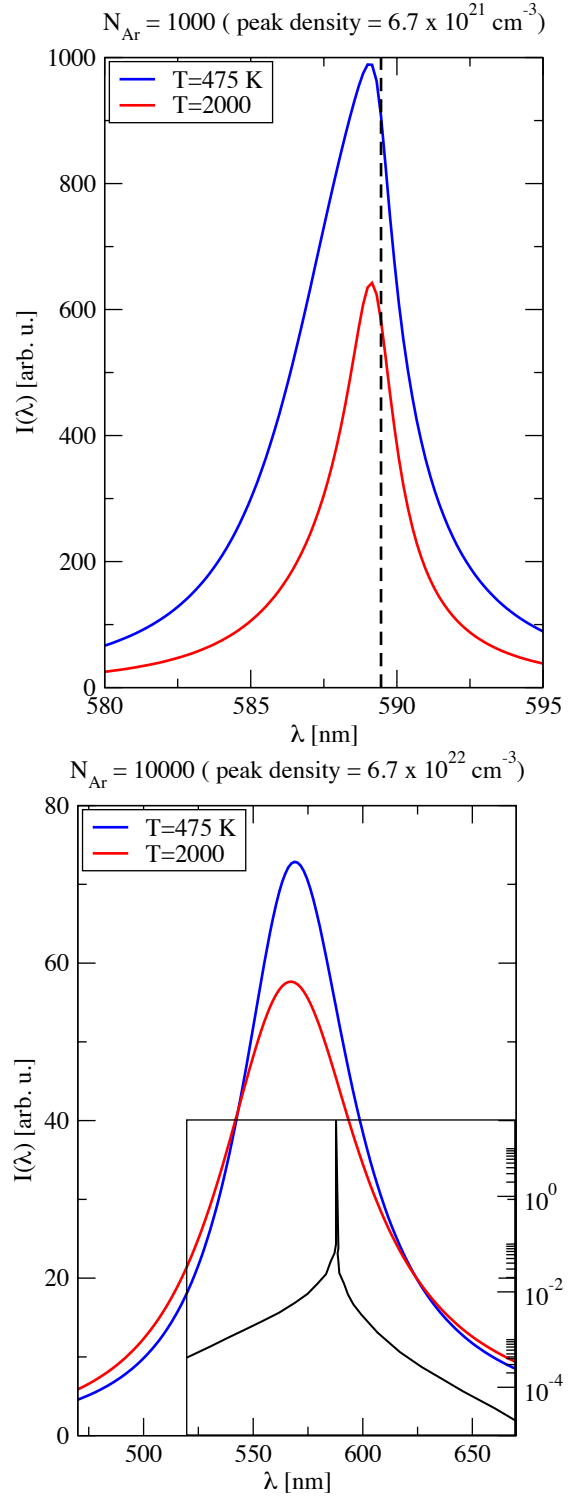


**Figure 3.** Temperature dependent spectral line profiles of Na D line embedded in an Ar haze of specific atomic/molecular density. Near the line center, the temperature dependent is the largest due to collisional effects, and away from the center, the lines are no longer Lorentzian as the temperature-insensitive mean field interaction potentials induce asymmetric lineshapes, e.g. Fig. 4. For comparison, we also show in the right figure inset the broadened line due to Na-He collision for which data is available (Burrows & Volobuyev 2003). The pressure broadening affects mainly the line center and, for the same density, is much narrower than the mean field broadened lines.

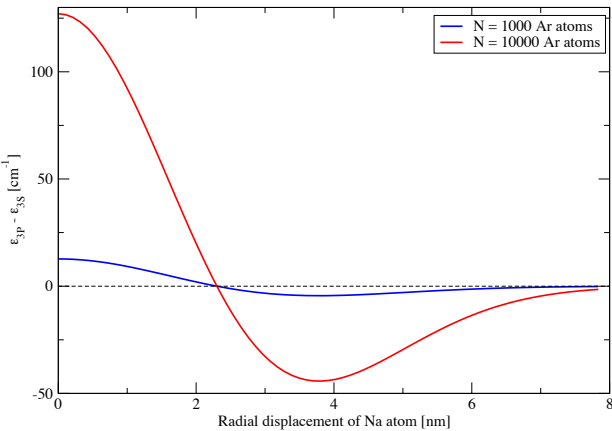


**Figure 4.** Distortion of the energy difference between levels Na(3S, 3P), due to Ar haze mean field, as a function of the position of the Na atom, for two different numbers of Ar atoms (peak densities  $p(R_r = 0)$  at  $R_r = 0$ ). The haze size parameter is  $a = 40 a_0$  (2.12 nm) in both cases, see Sec. 3.2, corresponding to peak densities of Ar atoms,  $6.7 \times 10^{21} \text{ cm}^{-3}$  and  $6.7 \times 10^{22} \text{ cm}^{-3}$  for  $N = 1000$  and  $N = 10000$ , respectively.

The averaged value of  $\Delta\omega$  in the haze-radiator interaction may be estimated from the mean field shift in Eq. 4:  $\hbar\Delta\omega \simeq \beta (2\pi L n_{\text{atomic}}^{haze} \hbar^2/m_e)$ . The numerical coefficient  $\beta$  shown in the front, scaling the mean field energy, can vary inside a broad interval  $0.1 \leq \beta \leq 1$  depending on the geometrical configuration of haze particles and the symmetry of the radiator electronic states. Examples of numerical calculations of the mean field energy shifts have been presented in Sec. 3. The ratio of cross sections in Eq. 7 depends on the number of atoms/molecules  $N$  in the haze particle and can be estimated as a ratio of the geometrical cross sections:  $\sigma_{\text{gas}}/\sigma_{\text{haze}} = 1/N^{2/3}$ . The haze impact on the atmospheric transit spectra is significant if  $\xi(\Delta\omega) \ll 1$ .

To illustrate the role of the haze-radiator interaction, we carry out a numerical estimate for  $\xi$  for Na radiation in an Earth-like atmosphere. The density of the atmospheric gas near location of the Na-layer could be taken as  $n_{\text{gas}} \sim 10^{14} \text{ cm}^{-3}$  with the haze particle density  $n_{\text{haze}} \sim 10^4 \text{ cm}^{-3}$ . This density of haze particles have been used recently for modeling of the exoplanetary transit spectra (Hörst & Tolbert 2013).<sup>1</sup> For small nano-size haze particles with  $N \sim 10^3$  we estimate the

<sup>1</sup> The typical density of Na atoms in the Earth Na layer is around  $10^4 \text{ cm}^{-3}$ . Ions of different metals Na, K, Fe, Mg, meteorite ashes, and nano-dust particles can be considered as centers of haze nucleation. In quasi-equilibrium conditions, the number density of haze particles should be relatively close to the layer density of metallic atoms and ions.

atomic density of these particles as  $n_{\text{atomic}}^{haze} \sim 10^{22} \text{ cm}^{-3}$ , with the Na atom velocity taken as  $v_r \sim 10^3 \text{ cm/s}$  and the gas collision cross section  $\sigma_{\text{gas}} \sim 10^{-15} \text{ cm}^2$ , and  $\beta \sim 0.1$ . For these conditions,  $\xi \sim 0.01 \ll 1$ , indicating a strong influence of haze particles on the spectral shape of atomic radiation and flattening of the Na-resonant spectral line.

The haze particles may also form layers, which can be separated from atmospheric metal layers. This separation leads to a significant reduction of the haze particle density  $n_{\text{haze}}$  in regions occupied by radiators and contributions of haze particles into formation of transit spectra can be negligible ( $\xi \gg 1$ ).

## 5. SUMMARY

In this work, a unified mean field framework for the spectral shift and broadening of an atomic radiator in a dense haze environment has been developed. Both collisional interaction, affecting the line center, and the mean field energy shifts due the presence of other atomic or molecular perturbers affecting the line wings, in hazy environments, are accounted for. The collisional contribution depends strongly on temperature and has a Lorentzian form, but the mean field shift is temperature insensitive. The line profiles in hazy environments are asymmetric and significantly broaden because the mean-field generated potential.

The current model has considerable flexibility for extension to different haze environments when chemical composition is mixed, particle densities vary from gaseous to solid phases, and variable porosities. The extension to carbon-bearing molecular haze requires a determination of the electron-molecule scattering length and the electronic wave functions for the molecule. Some values of the electron-molecule scattering length are available in the literature, e.g. for  $e^-$ -CH<sub>4</sub> (methane), the scattering length is about  $L = -2.9 a_0$  (McNaughten et al. 1990), for  $e^-$ -CO<sub>2</sub> (carbon dioxide), about  $L = -7 a_0$  (Fabrikant 1984), for  $e^-$ -C<sub>6</sub>H<sub>6</sub> (benzene), about  $L = -9.21 a_0$  (Field et al. 2001), and for  $e^-$ -C<sub>8</sub>H<sub>8</sub> (cubane), about  $L = -3.5 a_0$  (Gianturco et al. 2004), but the values depend sensitively on the properties of the molecule and application to specific chemistries will warrant careful analysis and possibly detailed scattering calculations.

The atomic radiator can be embedded within the haze, or outside and can radiate from atomic highly excited states, where strong line shift and broadening may inhibit excitations in the first place. The collisional shift and broadening can be quantitatively calculated at various temperatures with accurate quantum mechanical methods in the impact approximation (Vrinceanu et al.

2004). Our model can be extended to a description of the radiator embedded into liquid or solid matrix. The spectral lines obtained from the analysis above can be input in radiative transfer codes for proper modeling of the properties of the atmospheres and surface, such as

the Planetary Atmosphere Generator (Villanueva et al. 2018).

## 6. ACKNOWLEDGEMENTS

Z. F. was supported by an ITAMP faculty fellowship from an underrepresented institution. HRS and JFB were supported by an NSF grant to ITAMP. DV was supported by an NSF RISE grant to Texas Southern University.

## REFERENCES

Allard, N., & Kielkopf, J. 1982, *Rev. Mod. Phys.*, **54**, 1103

Boatz, J., & Mario, E. 1994, *J. Chem. Phys.*, **101**, 3472

Boys, S. F., & Bernardi, F. 1970, *Mol. Phys.*, **19**, 553

Burrows, A., Hubbard, W. B., Lunine, J. I., & Liebert, J. 2001, *Rev. Mod. Phys.*, **73**, 719

Burrows, A., Marley, M. S., & Sharp, C. M. 2000, *ApJ*, **531**, 438

Burrows, A., & Volobuyev, M. 2003, *Ap. J.*, **583**, 985

Burrows, A. S. 2014, *Nature*, **513**, 345

Deming, D., & Seager, S. 2017, ArXiv e-prints, [arXiv:1701.00493 \[astro-ph.EP\]](https://arxiv.org/abs/1701.00493)

Demkov, Y. N., & Ostrovskii, V. N. 1988, Zero-Range Potentials and Their Applications in Atomic Physics (Plenum Press, New York), 287

Encyclopaedia, T. E. P. 2018, The Extrasolar Planets Encyclopaedia, <http://www.exoplanet.eu/>

Explorer. 2018, Exoplanet Data Explorer, <http://www.exoplanets.org/>

Fabrikant, I. I. 1984, *J. Phys. B: At. Mol. Phys.*, **17**, 4223

Fermi, E. 1934, *Nuovo Cimento*, **11**, 157

Field, D., Ziesel, J.-P., Lunt, S. L., et al. 2001, *J. Phys. B: At. Mol. Opt. Phys.*, **34**, 4371

Fortney, J. J., Sudarsky, D., Hubeny, I., et al. 2003, *ApJ*, **589**, 615

Fuentealba, P., Preuss, H., Stoll, H., & Szentpály, L. V. 1982, *Chem. Phys. Lett.*, **89**, 418

Gianturco, F. A., Lucchese, R. R., Grandi, A., & Sanna, N. 2004, *J. Chem. Phys.*, **120**, 4172

Greenberg, J., & Li, A. 1999, *Space Sci. Rev.*, **90**, 149

Greene, C. H., Dickinson, A. S., & Sadeghpour, H. R. 2000, *Phys. Rev. Lett.*, **85**, 2458

Hörst, S. M., & Tolbert, M. A. 2013, *Ap. J. Lett.*, **770**, L10

Hörst, S. M., He, C., Lewis, N. K., et al. 2018, ArXiv e-prints, [arXiv:1801.06512 \[astro-ph.EP\]](https://arxiv.org/abs/1801.06512)

Jacquet, E., Zanuttini, D., Douady, J., & et al. 2011, *J. Chem. Phys.*, **135**, 174503

Jongerius, M., Bergen, A. V., Hollander, T., & Alkemade, C. 1981, *J. Quant. Spectrosc. Radiat. Transfer*, **25**, 1

Kreidberg, L., Bean, J. L., Désert, J.-M., et al. 2014, *Nature*, **505**, 69

Lendl, M., Cubillos, P. E., Hagelberg, J., et al. 2017, *A&A*, **606**, A18

Lenoble, J., Mishchenko, M. I., & Herman, H. 2013, In *Aerosol Remote Sensing* (J. Lenoble et al., Eds.), pp 13-51, 13

Marley, M. S., Ackerman, A. S., Cuzzi, J. N., & Kitzmann, D. 2013, *Clouds and Hazes in Exoplanet Atmospheres*, ed. S. J. Mackwell, A. A. Simon-Miller, J. W. Harder, & M. A. Bullock (Tucson: Univ. Arizona Press), 367

McNaughten, P., Thompson, D. G., & Jain, A. 1990, *J. Phys. B: At. Mol. Opt. Phys.*, **23**, 2405S

Morley, C. V., Fortney, J. J., Marley, M. S., et al. 2015, *Ap. J.*, **815**, 110

Nicklass, A., Dolg, M., Stoll, H., & Preuss, H. 1995, *J. Chem. Phys.*, **102**, 8942

Ortiz, J. L., Moreno, F., & Molina, A. 1996, *Icarus*, **119**, 53

Petrovic, Z. L., O’Malley, T. F., & Crompton, R. W. 1995, *Journal of Physics B: Atomic, Molecular and Optical Physics*, **28**, 3309

Pont, F., Knutson, H., Gilliland, R. L., Moutou, C., & Charbonneau, D. 2008, *MNRAS*, **385**, 109

Pont, F., Sing, D. K., Gibson, N. P., et al. 2013, *MNRAS*, **432**, 2917

Rannou, P., Hourdin, F., & McKay, C. 2002, *Nature*, **418**, 853

Saxon, R. P., Olson, R., & Liu, B. 1977, *J. Chem. Phys.*, **67**, 2692

Sciamma-O’Brien, E., Upton, K., & Salama, F. 2017, *Icarus*, **289**, 214

Seager, S., & Deming, D. 2010, *ARA&A*, **48**, 631

Seager, S., & Sasselov, D. D. 2000, *ApJ*, **537**, 916

Seignovert, B., Rannou, P., Lavvasa, P., & et al. 2017, *Icarus*, **292**, 13

Sing, D. K., Désert, J.-M., Fortney, J. J., et al. 2011, *A&A*, **527**, A73

Spake, J. J., Sing, D. K., Evans, T. M., et al. 2018, *Nature*, **557**, 68

Szasz, L. 1985, Pseudopotential theory of atoms and molecules (John Wiley and Sons, Inc., New York)

Szudy, J., & Baylis, W. 1996, *Physics Reports*, **266**, 127

Tinetti, G., Vidal-Madjar, A., Liang, M.-C., et al. 2007, *Nature*, **448**, 169

Tomasko, M. G., Karkoschka, J., & Martinek, S. 1986, *Icarus*, **65**, 218

Villanueva, G. L., Smith, M. D., Protopapa, S., Faggi, S., & Mandell, A. M. 2018, ArXiv e-prints, [arXiv:1803.02008](https://arxiv.org/abs/1803.02008) [astro-ph.EP]

Vinatier, S., Schmitt, B., Bazard, B., et al. 2018, *Icarus*, **310**, 89

Vrinceanu, D., Kotochigova, S., & Sadeghpour, H. R. 2004, *Phys. Rev. A*, **69**, 022714

Werner, H.-J., & P. J. Knowles *et al.* 2012, MOLPRO: a package of ab initio programs, version 2012.1

West, R. A. and Smith, P. H. 1991, *Icarus*, **90**, 330

Wong, A., Yung, Y. L., & Friedson, A. J. 2003, *Geophys. Res. Lett.*, **30**, 8

Zhang, X., Strobel, D. F., & Imanaka, H. 2017, *Nature*, **551**, 352 EP